REPORT DOCUMENTATION PAGE

Form Approved
OMB No. 0704-0188

1. REPORT DATE *(DD-MM-YYYY)*	2. REPORT TYPE	3. DATES COVERED *(From - To)*
	Technical Paper	

4. TITLE AND SUBTITLE

Please see attached

5a. CONTRACT NUMBER

5b. GRANT NUMBER

5c. PROGRAM ELEMENT NUMBER

6. AUTHOR(S)

5d. PROJECT NUMBER
2308

5e. TASK NUMBER
M13C

5f. WORK UNIT NUMBER
346057

7. PERFORMING ORGANIZATION NAME(S) AND ADDRESS(ES)

ERC

8. PERFORMING ORGANIZATION REPORT

9. SPONSORING / MONITORING AGENCY NAME(S) AND ADDRESS(ES)

Air Force Research Laboratory (AFMC)
AFRL/PRS
5 Pollux Drive
Edwards AFB CA 93524-7048

10. SPONSOR/MONITOR'S ACRONYM(S)

11. SPONSOR/MONITOR'S NUMBER(S)
Please see attached

12. DISTRIBUTION / AVAILABILITY STATEMENT

Approved for public release; distribution unlimited.

13. SUPPLEMENTARY NOTES

14. ABSTRACT

15. SUBJECT TERMS

16. SECURITY CLASSIFICATION OF:			17. LIMITATION OF ABSTRACT	18. NUMBER OF PAGES	19a. NAME OF RESPONSIBLE PERSON
a. REPORT	b. ABSTRACT	c. THIS PAGE	A		Leilani Richardson
Unclassified	Unclassified	Unclassified			19b. TELEPHONE NUMBER *(include area code)* (661) 275-5015

E01-047

MEMORANDUM FOR PRS (Contractor/In-House Publication)

FROM: PROI (STINFO) 20 December 2001

SUBJECT: Authorization for Release of Technical Information, Control Number: **AFRL-PR-ED-TP-2001-245**
B. Chehroudi (ERC), D. Talley, "Interaction of Acoustic Waves with a Cryogenic Nitrogen Jet at Sub- and Supercritical Pressures"

40th AIAA Aerospace Sciences Meeting & Exhibit **(Statement A)**
Reno, NV (14-17 Jan 2002) – (Deadline: 11 May 01)

1. This [illegible] been reviewed by the Foreign Disclosure Office for [illegible]

AIAA 2002-0342

Interaction of Acoustic Waves with a Cryogenic Nitrogen Jet at Sub- and Supercritical Pressures

B. Chehroudi and D. Talley#*

*Engineering Research Corporation Inc
10 E. Saturn Boulevard
Edwards AFB, CA 93524-7680

#Air Force Research Laboratory
Propulsion Directorate
10 E. Saturn Boulevard
Edwards AFB, CA 93524-7680

40th AIAA
Aerospace Sciences Meeting & Exhibit
14-17 January, 2002
Reno, Nevada

AIAA 2002-0342

Interaction of Acoustic Waves with a Cryogenic Nitrogen Jet at Sub- and Supercritical Pressures

B. Chehroudi[*] *and D. Talley*[#]

[*]Engineering Research Corporation Inc.
10 E. Saturn Boulevard
Edwards AFB, CA 93524-7680
(Corresponding author)

[#]Air Force Research laboratory
10 E. Saturn Boulevard
Edwards AFB, CA 93524-7680

Abstract

To better understand the nature of the interaction between acoustic waves and liquid fuel jets in rocket engines, cryogenic liquid nitrogen is injected into a room temperature high-pressure chamber having optical access on its sides. A piezo-siren capable of generating sound waves with an SPL of up to 180 dB is used under three chamber pressures of 1.46, 2.48, and 4.86 MPa. The reduced pressures for these pressures are 0.43 (subcritical), 0.73 (near-critical), and 1.43 (supercritical), respectively. The assembly consisting of the acoustic driver and the high-pressure chamber form a cavity that resonates at several frequencies, the strongest being at 2700 and 4800 Hz. Three different flow rates are considered and the nature of the aforementioned interaction has been documented via a high-speed imaging system using a CCD camera. It is found that the impact of the acoustic waves on the jet structure is strongest from low to near-critical chamber pressures and at low injectant flow rates. No significant effects of the acoustic waves are detected at the supercritical chamber pressure examined. It suggests that engine operation either near the critical point or in transition passing through the critical point could be troublesome and may lead to or feed combustion instabilities in liquid rocket engines. Further work is needed to directly relate these effects to the observed instabilities.

Introduction

Combustion instability has always been one of the most complex phenomena in liquid rocket engines, and therefore difficult to fully control particularly in the design of large output rockets. These difficulties stem from the emergence of oscillatory combustion with large pressure amplitudes. In one classification, high-amplitude, low-frequency (less than several hundred Hertz) pressure variations (or chugging) due to combustion is understood to be coupled with the feed line and structural modes of oscillations. Chugging is responsive to system-type analysis. Another instability is characterized by high amplitudes and high frequencies (screaming), and can lead to local burnout of the combustion chamber walls and injector plates (acoustic instability). This is caused by extreme heat-transfer rates brought about by high-frequency pressure and gas velocity fluctuations, see *Harrje and Reardon [1]*.

Two types of instabilities have been recognized in the past: linear instability, also called spontaneous or self-triggered, and nonlinear instability (or dynamic instability). Dynamic instability refers to a linearly stable system that becomes nonlinearly unstable in response to a sufficiently large disturbance. The underlying mechanism is the widely cited general principle by *Lord Rayleigh [2]*. In essence, he stated that the interaction between the combustion heat release and the acoustic field is the strongest if heat is added in a region of space and at the time when the acoustic amplitude is the highest. Although this view has been useful, overwhelming evidence gathered by past investigations attributed combustion instability to a complex interaction of the external acoustic field with the fuel injection processes, thereby leading to incidences of instability in rocket engines. For this and other reasons, controlled studies have been conducted probing into the effects of acoustic waves on gaseous and liquid jets from a variety of injector hole designs. A series of investigations concentrated on disturbances induced from within the injection system. They considered the effects of acoustic fields on many phenomena such as flow structure, vortex pairing, and shear layer growth rate in the initial region of the jet (for example, see a short review article by *Kiwata, et al. [3]*). More relevant to the work reported here, are a few reports and articles on gaseous or (in particular) liquid jets under the influence of external (transverse and longitudinal) acoustic fields. Although both longitudinal and transverse acoustic mode instabilities exist in rocket engines, for at least two reasons longitudinal modes are more stable. First, the exhaust nozzle provides heavier damping for the longitudinal modes than the tangential modes. Second, near-injector processes in the thrust chamber are generally more sensitive to velocity fluctuations parallel to the injector face than normal to it, see *Oefelein and Yang [4]*. Those investigations using external acoustic disturbances can be divided into two subgroups based on the state of the injected fluid, i.e., gaseous or liquid. In the following, selected works of immediate relevance to ours will be briefly described with more focus on those employing transverse acoustic waves

with a particular attention to liquid phase injection systems.

To provide maximum effects, *Miesse [5]* used two opposing localized acoustic drivers 180 degrees out of phase to investigate the impact of a transverse acoustic field on a low velocity liquid jet ($10 < L/d < 40$) at atmospheric chamber pressure. Images showed that the amplitude of the jet dispersion decreased with an increase in both the frequency (less than 200 Hz was used) of the driver and pressure drop across the injector (i.e. flow rate). It was also noted that the sound field considerably reduced the length of the solid stream. Maximum dispersion was observed at the natural frequency of the jet defined as approximately 0.029U/d, where U and d are mean jet velocity and diameter respectively.

Buffum and Williams [6] considered the interaction of external transverse acoustic waves at frequencies ranging from 100 to 500 Hz on a liquid turbulent jet at atmospheric pressure. The main physical quantity measured was the oscillatory displacement of the liquid jet as it passed through an acoustic standing wave field in a resonant tube. Using a closed tube and driving it at its fundamental resonant frequency, sinusoidal acoustic intensities up to about 160 dB were obtained. Resonance effects at different frequencies were achieved through variations of the tube length in this study. It was found that the peak-to-peak jet deflection decreased when jet diameter or velocity was increased due to increased fluid mass in the acoustic field. The jet deflection was unobservable below 130 dB and ummeasurable below 140 dB. Shearing atomization began at about 161 dB and was proposed to cause sizable periodic reactant sources to sustain or amplify combustion instabilities. Also, they measured higher drag coefficients for turbulent liquid jets in transverse acoustic fields and found them to be an order of magnitude larger than that of a solid cylinder having a diameter the same as that of the injector orifice. This caused enhanced jet deflections in the acoustic field and may be one source for sustaining the instability in liquid rocket engines.

Heidmann and Groeneweg [7] considered the effects of transverse traveling and standing acoustic waves (5 to 20 % of the mean chamber value) on both a single round jet (liquid oxygen burning with gaseous hydrogen) and an impinging jet. The time varying jet length was observed to be coupled with the acoustic field which raised the suspicion that unstable combustion was directly related to the dynamic behavior of the liquid jet. From the observations in the impinging jets (nitrogen oxides and hydrazine), they stated that nonlinear instability occurred when the acoustic oscillations were of sufficient magnitude to cause jet breakup before the impingement point. The severity of this nonlinear instability was reduced by protecting the jets with thin walled tubing and thus maintaining impingement.

A work in which transverse disturbances generated by an oscillating plate at a fixed amplitude but different frequencies (1000 to 10000 Hz) is also of interest here. A relatively large planar nozzle was used by *Rockwell [8]* to inject water and investigate the details of vortex formation and their interactions near the exit area. The effects of the frequency of oscillations on the natural vortex coalescence was classified based on a Strouhal number ($St=fd/U$, where f, d, and U are the excitation frequency, jet diameter, and mean jet velocity) versus Reynolds number ($Re=\rho Ud/\mu$, where ρ and μ are the injectant density and viscosity) plot. For the range of Re investigated (1860 to 10800), natural breakdown of the jet (with no external disturbance) was observed to within a few nozzle widths. The dimensionless frequency (St_N) was found to change with Re as $St_N = 0.012\ (Re)^{0.5}$. *Becker and Massaro [9]* also found the same value for axisymmetric air jets for Reynolds number ranging from 1,000 to 10,000. Four regimes were distinguished based on the observed effects of the external disturbance on the nature of the vortex interaction. The reference regime was that corresponding to the natural breakdown of the jet. The four regimes were named, in order of decreasing St number, "upper zone," "preservation," "matched excitation," and "forced fusion" regimes. A plot of these regimes will be given later and compared with the values estimated in our study, see Fig. 11. In the upper zone regime where the excitation frequencies were higher than about 3 to 4 times the natural breakdown frequency ($St > 3\ St_N$) no effects were observed. In the preservation regime, the core flow of the jet tended to be preserved followed by the induction of smaller vortices, the time-averaged velocity profile was narrowed, and the longitudinal turbulence was decreased (relative to undisturbed case). When the excitation frequency was matched with the natural breakdown frequency (matched regime), the effect was to accelerate the process of vortex formation and growth relative to the undisturbed case. Also, transverse distortion of the jet core was seen due to the vortex growth and coalescence. For the symmetrical jet work of *Becker and Massaro [9],* symmetrical ring vortices were produced and highest time-averaged widening of the jet occurred. This was in contrast to the planar jet case in which vortices on the two sides of the jet were 180 degrees out of phase with each other. This regime merges to the preservation regime at higher Re number (~ 10,000). In the forced fusion regime (frequencies ~1/3 of natural jet breakdown), the natural breakdown vortices were forced to fuse early as a result of the formation of large-diameter applied disturbance vortices. *Vaslov and Ginevskiy [10]* found that in this regime the time-averaged velocity profile of the jet was broadened. Finally, in the lower zone regime, (frequencies < 1/10 of natural jet breakdown) the vortex growth was unaffected in their formation region. In the limit, however, as St approaches zero, the jet experienced a quasi-steady deflection process. *Rockwell [8]* stated that a fallacious averaged jet widening is detected if a time-averaged measurement technique is used downstream the injector, when in reality the jet is being deflected by the applied transverse disturbance.

We therefore have a preponderance of evidence pointing at the important role played by the near injector phenomena and their interaction with the acoustic waves in combustion instabilities observed in rocket engines. Considering the forgoing, it is clear that although useful information has been collected in the past, there is a large gap in information regarding the effects of the acoustic waves on turbulent jets under more realistic conditions relative to liquid rocket engines. Knowledge on the effects of acoustic waves under high ambient pressure and in particular under near- and super-critical pressures is lacking. To this end, experimental research has been undertaken at the Air Force Research Laboratory (AFRL) to investigate the impact of acoustic waves under high pressures ranging from subcritical to supercritical pressures. To our knowledge, this is the first time such an interaction has been studied. This work extends the previous activities of the group on supercritical jet breakup phenomena of relevance to cryogenic liquid rocket engines, see *Chehroudi et al. [11,12,13].*

Experimental Setup

To better understand the nature of the interaction between acoustic waves and injected liquid fuels in rocket engines, cryogenic liquid nitrogen is injected into a room temperature high-pressure chamber with full optical access on its four sides. Figure 1 shows a schematic diagram of the experimental rig. The stainless steel chamber can withstand pressures and temperatures of up to 20 MPa and 473 K, respectively. It has two facing circular sapphire windows for optical diagnostics. Liquid N_2 is used to cool and/or liquefy the injectant passing through the cryogenic cooler prior to injection. The mass flow rate of the injectant is measured and regulated via a mass flowmeter, and a precision micrometer valve. Back-illumination of the jet

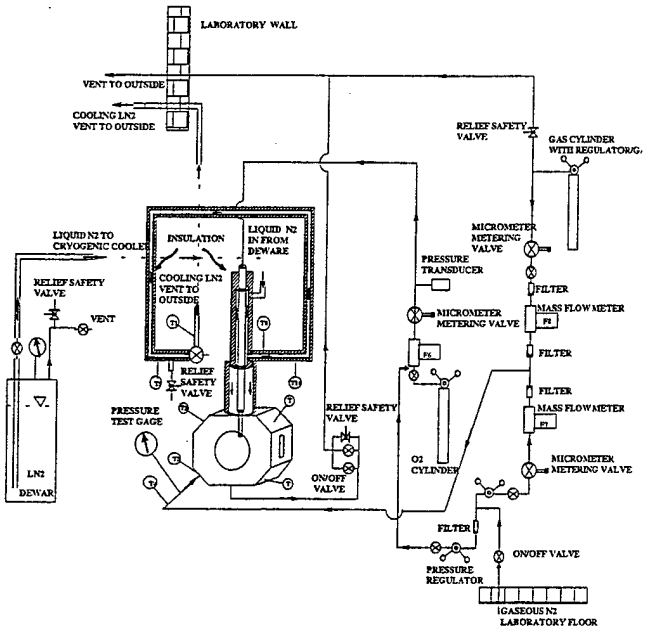

Figure 1. Schematic diagram of experimental setup for sub- to supercritical jet injection

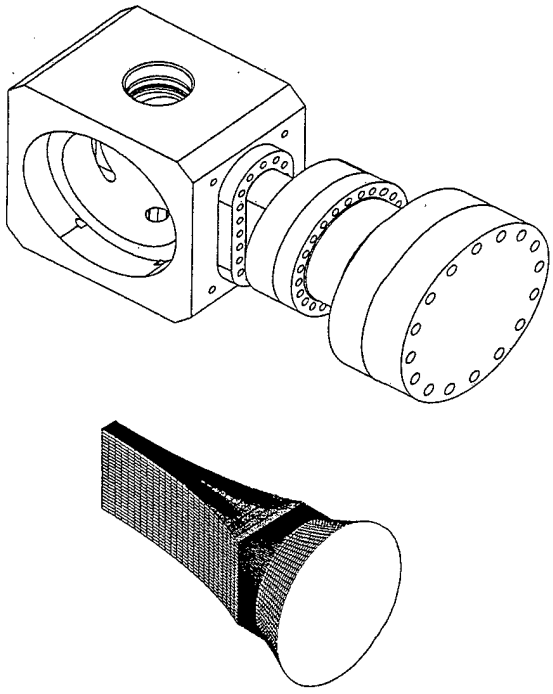

Figure 2. Top: coupling of the acoustic driver (piezo-siren) with the high-pressure chamber. Bottom: the design of the circular-to-rectangular channel to guide the waves into the chamber.

is accomplished with diffuse light flashes (0.8 μs duration). A model K2 Infinity long distance microscope is used with a high resolution (1280(H) x 1024(V) pixels in an 8.6(H)x6.9(V) mm actual sensing area with a pixel size of 6.7μm x 6.7 μm) CCD camera by the Cooke Corporation to form images of the injected jets. For the results reported, the cryogenic jet is injected through a sharp-edged stainless steel tube having a length, L of 50 mm, and inner and outer diameters measuring d_i = 0.254 mm and d_o = 1.59 mm, respectively. The resulting L/d_i was 200, which is sufficient to ensure fully developed turbulent pipe flow at the exit plane. The Reynolds number in these studies ranges from 14,000 to 80,000. The rig is fully instrumented to measure pressure, temperature, and mass flow rate of the injected fluid. A specially designed piezo-siren by Hersh Acoustical Engineering, Inc., capable of producing sound pressure levels (SPL) of up to 180 dB (in an impedance tube) at its resonant frequencies (lying between 1000 to 8000 Hz) and at pressures up to 2000 psi is used with a circular-to-rectangular transition coupling to bring the acoustic waves into the interaction zone inside the chamber. The SPL is defined as $20\log(P_e/P_{e,\,ref})$ where P_e is the RMS of the pressure oscillations and the reference pressure is 20.4 μPa. For example, a 1 psi amplitude of the sinusoidal fluctuations is equivalent to 167.4 dB. A model 601B1 Kistler piezoelectric-type pressure transducer is used to measure the acoustic pressure variations inside the chamber at various pressures very near the jet location. The piezo-siren acoustic driver is

able to generate between 161 to 171 db when coupled with the high-pressure chamber.

A Summary of Previous Results on Supercritical Jets at AFRL

During the past three years, results from the injection of several fluids into an ambient under both sub- and supercritical pressures at sufficiently high Reynolds numbers to be considered as fully-turbulent flow have been reported for the same test facility shown in Fig.1, see *Chehroudi et al. [11]*. A variety of ambient fluids was used into which pure N_2, He, and O_2 fluids were injected. The effects of chamber pressure (density) ranging from thermodynamic subcritical to supercritical pressures at a supercritical chamber temperature (based on the critical pressure and temperature, P_c, T_c, of the injectant) were observed by the acquisition of shadowgraph images from the injector exit region using a CCD camera illuminated by short-duration light pulses.

At sufficiently low subcritical chamber pressures, the disturbances on the jet interface amplified downstream and eventually broke up into irregularly-shaped small entities. A further increase of chamber pressure initiated the formation of many small ligaments and droplets at the interface of the jet only within a narrow regime below the thermodynamic critical pressure of the injected pure fluid, resembling a second wind-induced liquid jet breakup. At even higher chamber pressures, near but below the critical pressure of the injectant, the expected transition into a full atomization regime to produce a liquid spray was inhibited due to reduction of both the surface tension and the heat of vaporization. The jet appearance changed abruptly at this pressure and resembled that of a turbulent gas jet for all higher chamber pressures. The initial growth rate of the jet was plotted together with available data on liquid fuel injection in diesel engine environments, and turbulent incompressible, supersonic, and variable-density jets and mixing layers. The resulting plot is unique in its own right, covering four order of magnitude in density ratio. At near- and super-critical pressures, these measurements agreed well with the theoretical growth rate equations proposed *by Brown [14], Papamoschou and Roshko [15],* and *Dimotakis [16]* for incompressible but variable-density turbulent mixing layers. This constituted the first quantitative evidence in support of the past qualitative observations that the jet appeared to evolve into a gas-like behavior under supercritical condition. The geometry of the jet interface was also examined for the first time by fractal analysis. The results clearly indicated a transition from a Euclidean to a fractal interface, with a fractal dimension close to values measured for gaseous turbulent jets. This provided an additional quantitative evidence for the hypothesis that the jet evolved into a gas-like behavior. An equation was proposed based on a physical model proposing that at the point of transition from liquid-like to gas-like appearances and growth rates, the characteristic time of the vaporization process is of the same order as that of the interfacial "bulge" formation/separation events. The model equation agreed well with the experimental growth rate data. Finally, The initial growth rate of the jet as judged by the Raman signature was in reasonably good agreement with our earlier measurements using shadowgraphy if twice the full width half maximum (FWHM) of the normalized intensity plots was used, *see Chehroudi et al. [17].*

Experimental Results

It is found that a certain minimum oscillation amplitude is needed to bring about a detectable interaction. When a rapid transition is made from below to above this minimum value, a strong and transitory effect is observed, characterized by eruption of many drops and ligaments from the surface of the jet combined with amplification of the surface wave instabilities. When set at its highest achievable acoustic wave amplitude, the oscillation augmented the unstable surface waves and imposed a zigzag-shaped contour to the jet. Preliminary results under subcritical condition indicates constriction of the jet in the acoustic propagation direction (perpendicular to the jet axis) near the injector exit followed by the acceleration of the atomization process further downstream. Figures 3, 4, and 5 shows effects of acoustic waves (traveling from left to right in these figures) on the liquid nitrogen jet at three different flow rates and at subcritical, near-critical, and supercritical pressures, respectively. Each composite jet image consists of a mosaic of several images taken from the same test run but at different times and jet axial locations. At each axial position up to 10 images were taken. These images were not taken at any specific phase with respect to the acoustic driver. The acoustic coupling guide and the high-pressure chamber form a cavity that resonates at certain distinct frequencies. Under the current setup, the highest amplitude of pressure oscillations can be detected at only two frequencies (~ 2700 and ~ 4800 Hz). Considering a speed of the sound of about 357 m/s, the acoustic wavelength is 13.1 and 7.4 cm/s when the driver oscillates at 2700 and 4800 Hz, respectively. This value is much larger than the jet diameter investigated here. Figures 3, 4, 5 are taken when the acoustic piezo-siren was driven at about 4800 Hz. Similar images were collected at 2700 Hz but are not shown here. However, the general wave/jet interaction effects are the same at these two frequencies.

Reduced Pressure Pch/Pc , Pc is critical Pressure	Chamber Pressure Pch, MPa	LN2 FLOW RATE, mg/s 150	300	500
		REYNOLDS # ESTIMATE		
0.43	1.46	14323	33674	47742
0.73	2.48	20489	48172	68296
1.43	4.86	24816	59771	82721

Table1. Estimates of the Reynolds numbers at different injectant flow rates.

Dramatic effects of the acoustic field on the jet structure, particularly at low flow rates and near-critical conditions can easily be seen at a first glance. Also, the narrowing of the jet is apparent near the injector exit region, as though it is pinched in the acoustic wave direction. The jet intact length is shortened and consequently a larger amount of mass is evaporated as compared to the unexcited jet (see the case for the lowest flow rate in Figs. 3 and 4). At the lowest flow rate the jet is seen to have been deflected in the mean sense in the direction of acoustic wave propagation, see Fig. 3. However, these effects are hardly detectable at supercritical pressures, see Fig. 5. Inspection of Figs. 6, 7, and 8, taken perpendicular to the direction shown in Figs. 3, 4, and 5, clearly indicates strong effects of the acoustic waves on spreading the liquid nitrogen mass in the direction perpendicular to the acoustic wave propagation. These images were taken on a different test run than those shown in Figs. 3, 4, and 5. However, the operating conditions were as close as possible to those in the previous figures. Although not shown here, the general behavior is similar when the acoustic driver was driven at 2700 Hz.

The impact of the acoustic waves on the jet is reduced as inertia forces increase through an increase of flow rate. This is similar to the observation of Buffum and Williams [6]. To extract some quantitative information from these images, a distance from the injector exit plane is selected within the first frame of the composite images shown in Figs. 3 to 8. This axial distance was at about 5 injector diameters in order to be representative of the effects in the initial region of the jet. Horizontal-row pixel information for a region of one injector diameter in the axial direction is averaged to extract a jet thickness value. Also, the information for up to 10 injector diameters is used to measure the initial jet spreading angle. For each case the average of 10 images was used for these calculations. Results from these measurements are shown in Figs. 9 and 10. A thickness of about 90 pixels in these figures represents one injector hole diameter. This can be seen for data taken at the lowest chamber pressure. The data with and without acoustic waves were taken back-to-back and from the same run. The contraction of the jet in the acoustic direction can be seen in Figs. 9(a) and (b) particularly at 2700 Hz. The strongest expansion of the jet is measured at low flow rates and low to near-critical chamber pressures, being highest at near-critical pressures. This observation is also supported by inspection of the data in Fig. 10. As proposed by others, this enlarged impact of the acoustic waves near the critical point of the injectant can be one important underlying reason for combustion instability in liquid rocket engines.

The situation for supercritical jets is quite different. Minimal effects of the acoustic waves on jet structure or its spread rate is seen. To search for some plausible reason, we use the information that at supercritical pressures, the unperturbed jet spreading rate is the same as an incompressible variable-density gaseous jet, see *Chehroudi et al. [11]*. For this reason, one expects existence of vortices similar to what has been described, for example, by *Rockwell [8]*. To investigate this matter further, our supercritical data is superimposed on a plot by him indicating different regimes discussed in the introduction section. Figure 11 shows a plot of the Strouhal number as a function of the Reynolds number. The curve marked "matched excitation" is the same equation proposed by *Becker and Massaro [9]* for the natural breakdown of the jet. Results from current study is beyond the regions studied before and one should beware of the dangers of extrapolation. Fortunately, the extrapolation is not too far from those reported in Fig. 11. Figure 11 suggests that the frequencies used here are not expected to bring about noticeably large effects of the acoustic waves because they lie in the region identified by *Rockwell [8]* as the "lower zone." No effects of the transverse disturbance on the jet were observed in the studies conducted by *Rockwell [8]* in this regime as described in the introduction section. Note that the lowest flow rate case tends to enter into the "forced fusion" regime where stronger interaction is expected, see Fig. 11.

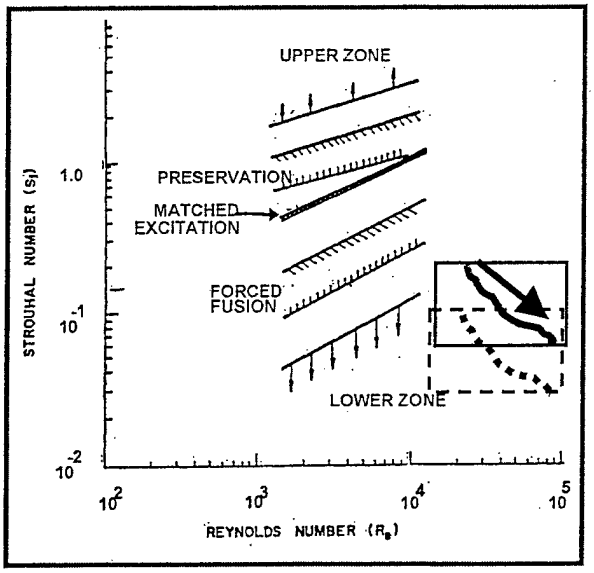

Figure 11. Regimes discussed by *Rockwell [8]* shown on an excitation Strouhal number versus the jet Reynolds number plot. The small solid rectangle to the right indicates the approximate region in which the current study lies when excitation is at 4800 Hz. The curve in this rectangle shows the approximate path as flow is increased from the lowest to the highest. Similar region for the 2700 Hz excitation is shown as a dashed rectangle.

Summary and Conclusions

Cryogenic nitrogen is injected into a chamber filled with gaseous nitrogen at room temperature which can support controlled acoustic waves. These waves are generated via mechanical vibration of a plate by a piezoelectric material. The chamber resonates at certain distinct frequencies found to be suitable for this study due to its high amplitude oscillations. At the lowest chamber pressure tested here (subcritical), the jet is strongly affected by the

waves. As the flow rate is increased, the inertia forces become very large and the observed interaction is substantially weakened. Operation of the chamber at near the critical pressure profoundly affected the jet structure, bringing early breakup and dispersion of the jet. Again, this effect is subdued at higher flow rates. At a supercritical chamber pressure, the effects of the acoustic field on the jet becomes unnoticeable. Due to its gas-jet like behavior, the supercritical jet is assumed to posses similar vortex formation and coalescence observed in turbulent jets, as reported by *Rockwell [8]*. Comparison to his results showed that the excitation St number used in the current work is too low to bring about any noticeable effects in the initial region of the jet.

Acknowledgement

Mr. Mike Griggs, Mr. Earl Thomas, and Mr. Randy Harvey are thanked for their valuable support. Ms. Jennie Paton and Ms. Tony Collett are to be especially thanked for making the requested literature available in a timely manner. We also appreciate Mr. Kevin Bradley's contribution in part of the data acquisition and processing. Dr. Rich Cohn is thanked for kindly offering his expertise in image acquisition area. This work is sponsored by the Air Force Office of Scientific Research, Dr. Mitat Birkan, program manager.

References

1. Harrje, T. D. and Reardon, H. F., Liquid Propellant Rocket Combustion Instability, NASA report number NASA SP-194, 1972.

2. Rayleigh, Lord, "The Explanation of Certain Acoustical Phenomena," *Royal Institution Proceedings*, vol. VIII, London, 1878, pp. 536-542.

3. Kiwata, T., Okajima, A., and Ueno, H., "Effects of excitation on plane and coaxial jets," Proceedings of the 3rd Joint ASME/JSME Fluid Engineering Conference, July 18-22, San Francisco, California, 1999.

4. Oefelein J. C. and Yang, V., "Comprehensive Review of Liquid Propellant Combustion Instabilities in F-1 Engines, *Journal of Propulsion and Power*, Vol. 9, No. 5, 1993, pp.657-677.

5. Miesse, C. C., The Effect of Ambient Pressure Oscillations on the Disintegration and Dispersion of a Liquid Jet," *Jet Propulsion*, 25, pp. 525-530, 534, 1955.

6. Buffum, F. G., and Williams, F. A., "Response of Turbulent Liquid Jets to Transverse Acoustic Fields," Proceedings of the 1967 Heat Transfer and Fluid Mechanics Institute, Edited by P. A. Libby, D. B. Olfe, and C. W. Van Atta, 1967, pp. 247-276, 1967.

7. Heidmann, M. F. and Groeneweg, J. F., "Analysis of the Dynamic Response of Liquid Jet Atomization to Acoustic Oscillations," NASA Technical Note, NASA TN D-5339, July, 1969.

8. Rockwell, D. O.," External Excitation of Planar Jets," *Journal of Applied Mechanics*, pp. 883-891, December 1972.

9. Becker, H. A. and Massaro, T. A., "Vortex Evolution in a Round Jet," *Journal of Fluid Mechanics*, Vol. 31, Part 3, pp.435-448, 1968.

10. Vaslov, Ye. V. and Ginevskiy, A. S., "Acoustic Effects on Aerodynamic Characteristics of a Turbulent Jet," Foreign Technology Division, Air Force Systems Command, No. FTD-MT-24-232-68, Aug., 1968.

11. Chehroudi, B., Talley, D.G., and Coy, E., "Fractal Geometry and Growth Rate Changes of Cryogenic Jets Near the Critical Point," 35th AIAA/ASME/SAE/ASEE Joint Propulsion Conference and Exhibit, paper AIAA 99-2489, 20-24 June, Los Angeles, CA, 1999.

12. Chehroudi, B., Cohn, R., and Talley, D.G., "Cryogenic Shear Layers: Experiments and Phenomenological Modeling of the Initial Growth Rate Under Subcritical and Supercritical Conditions," *International Journal of Heat and Fluid Flow*, to appear (2002).

13. Chehroudi, B., Cohn, R., and Talley, D.G., "Visual Characteristics and Initial Growth Rates of Round Cryogenic Jets at Subcritical and Supercritical Pressures," *Physics of Fluids*, vol. 14, no. 2, February, 2002.

14. Brown G., "The Entrainment and Large Structure in Turbulent Mixing Layers," 5th Australasian Conf. on Hydraulics and Fluid Mech., 1974, pp. 352-359.

15. Papamoschou, D. and Roshko, A. "The Compressible Turbulent Shear Layer: an Experimental Study," *Journal of Fluid Mechanics*, vol. 197, 1988, pp. 453-477.

16. Dimotakis, P. E. "Two-Dimensional Shear-Layer Entrainment," *AIAA Journal*, 21, No. 11, 1986, pp. 1791-1796.

17. Chehroudi, B., Cohn, R., Talley, D., and Bakakhshan, A., "Raman Scattering Measurements in the Initial Region of Sub- and Supercritical Jets," 36th AIAA/ASME/SAE/ASEE Joint Propulsion Conference, paper AIAA-2000-3392, 17-19 July, 2000.

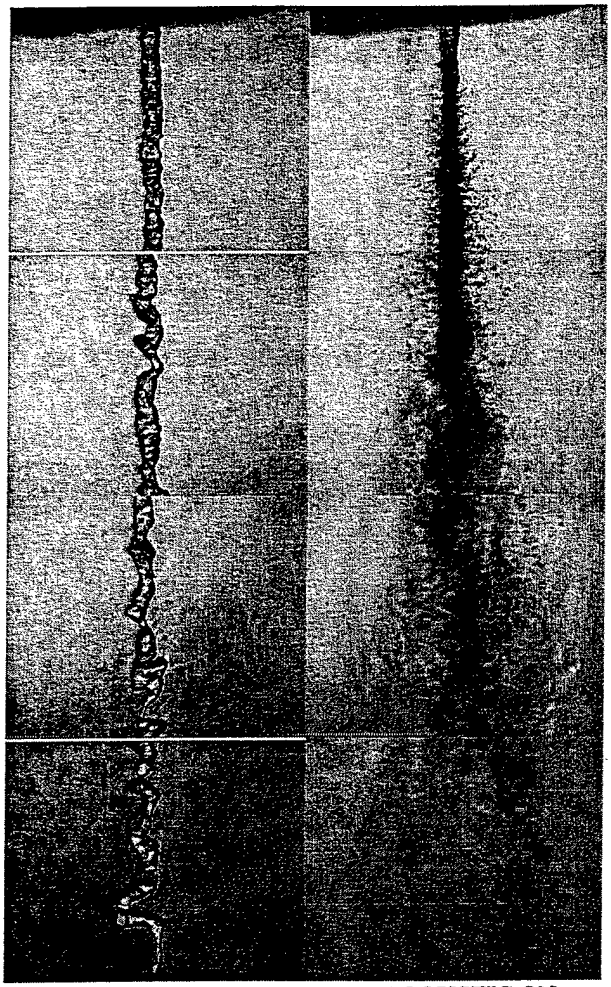

NORMAL ACOUSTIC ON
4800/1.46 /150 FRONT

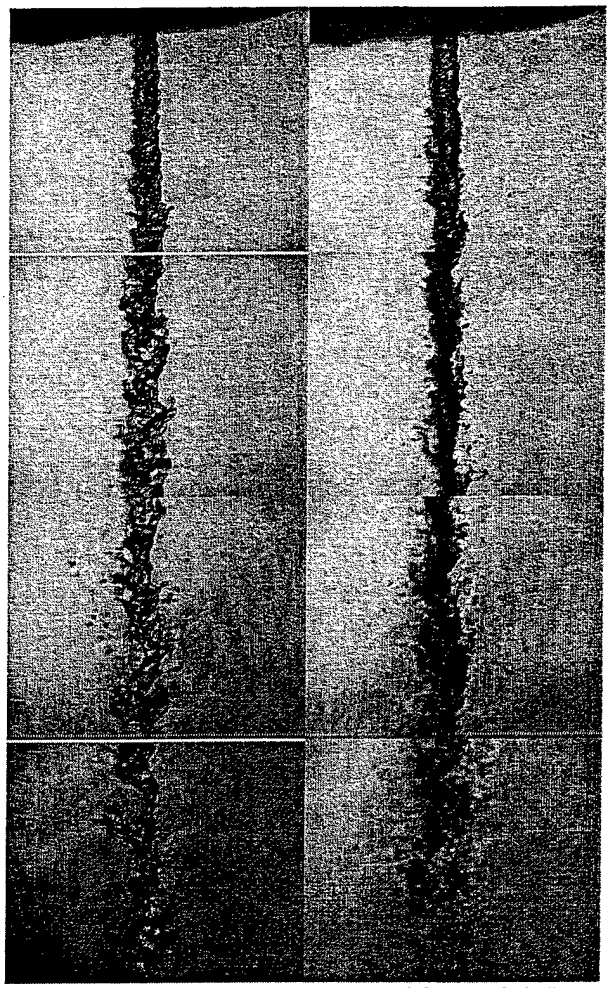

NORMAL ACOUSTIC ON
4800/1.46 /500 FRONT

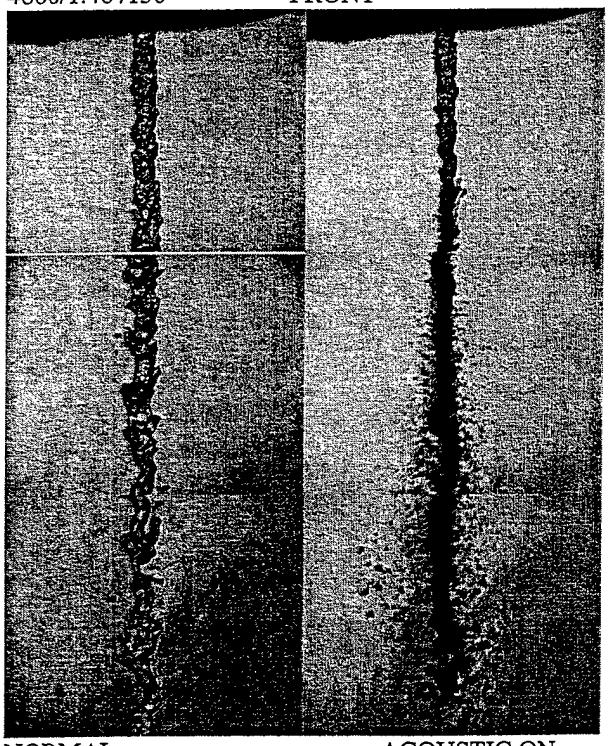

NORMAL ACOUSTIC ON
4800/1.46 /300 FRONT

Figure 3. Images of the liquid nitrogen jet injected into the gaseous nitrogen chamber at a subcritical chamber pressure of 1.46 MPa and three different injected flow rates of 150, 300, and 500 mg/s. Acoustic waves are traveling from left to right in these images. The acoustic wave frequency was set at 4800 Hz. Each composite jet image consists of a mosaic of several images taken from the same run but at different times and jet axial locations.

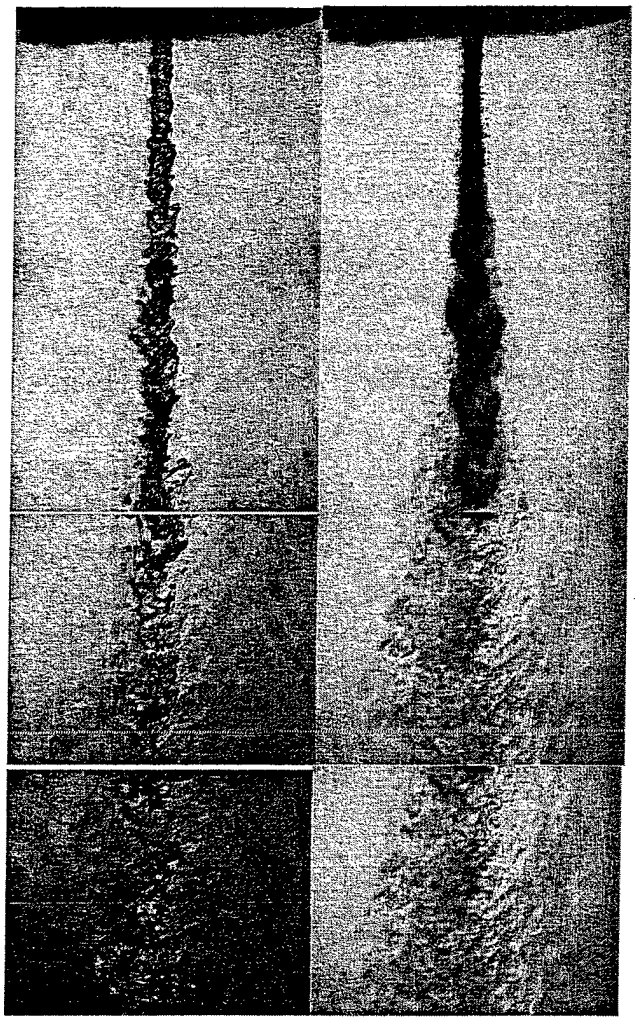

NORMAL ACOUSTIC ON
4900/2.48/150 FRONT

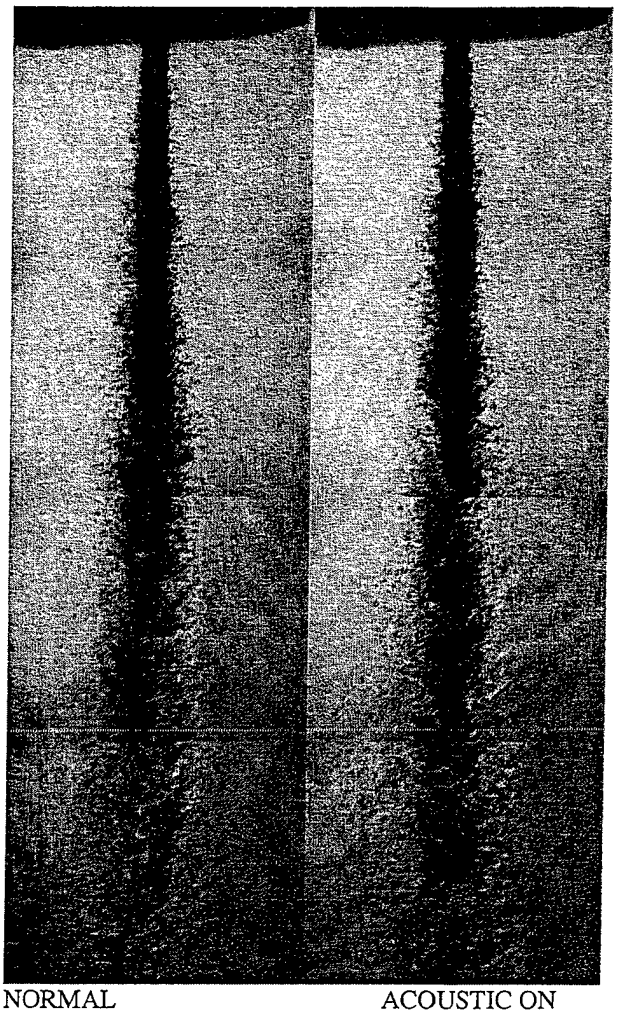

NORMAL ACOUSTIC ON
4900/2.48/500 FRONT

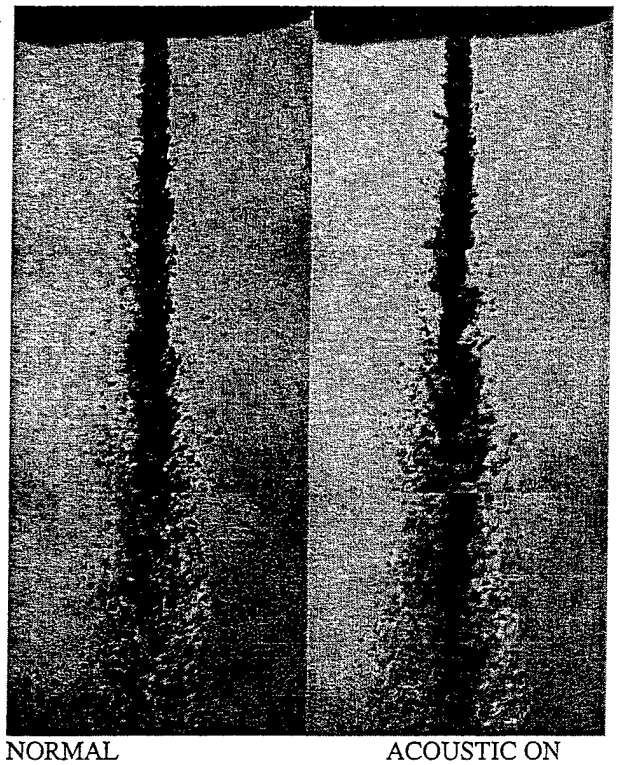

NORMAL ACOUSTIC ON
4900/2.48/300 FRONT

Figure 4. Images of the liquid nitrogen jet injected into the gaseous nitrogen chamber at a near-critical chamber pressure of 2.48 MPa and three different injected flow rates of 150, 300, and 500 mg/s. Acoustic waves are traveling from left to right in these images. The acoustic wave frequency was set at 4900 Hz. Each composite jet image consists of a mosaic of several images taken from the same run but at different times and jet axial locations.

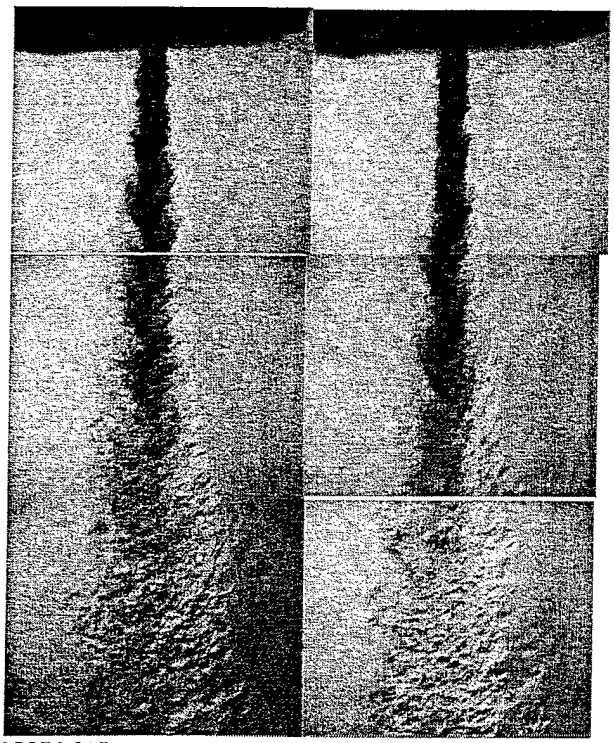

NORMAL ACOUSTIC ON
4800/4.86/150 FRONT

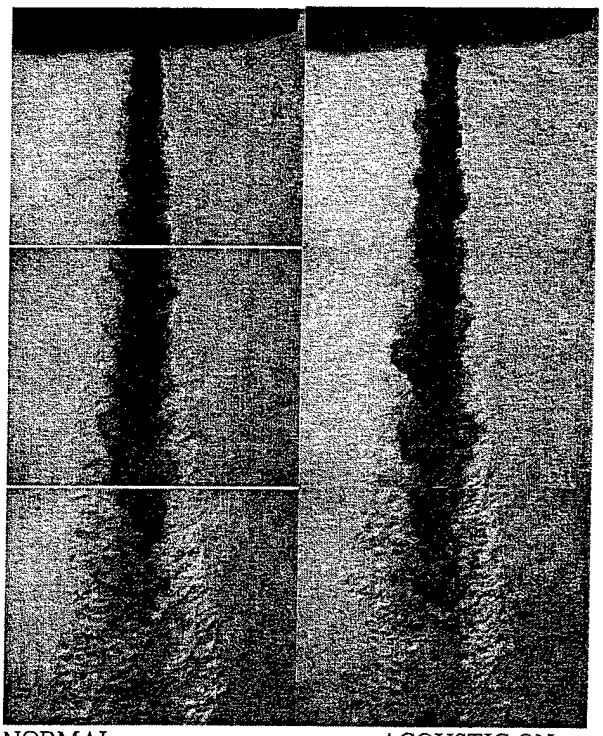

NORMAL ACOUSTIC ON
4800/4.86/500 FRONT

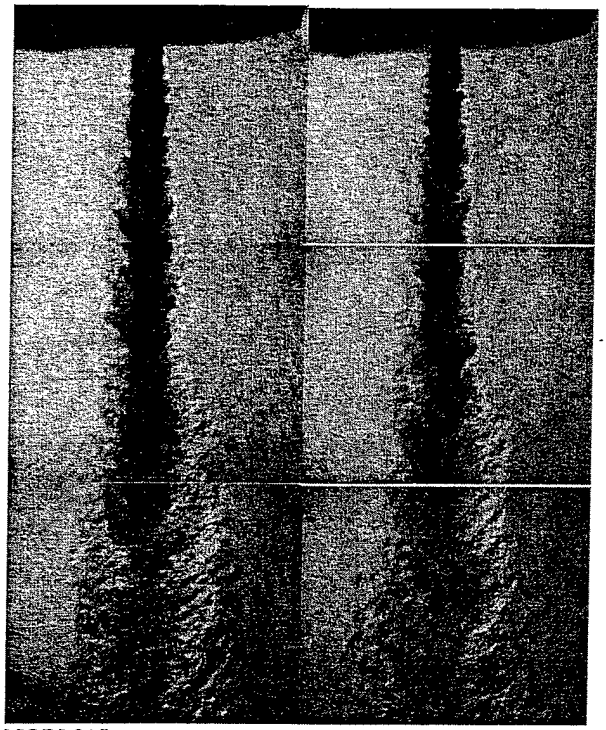

NORMAL ACOUSTIC ON
4800/4.86/300 FRONT

Figure 5. Images of the liquid nitrogen jet injected into the gaseous nitrogen chamber at a supercritical chamber pressure of 4.86 MPa and three different injected flow rates of 150, 300, and 500 mg/s. Acoustic waves are traveling from left to right in these images. The acoustic wave frequency was set at 4800 Hz. Each composite jet image consists of a mosaic of several images taken from the same run but at different times and jet axial locations.

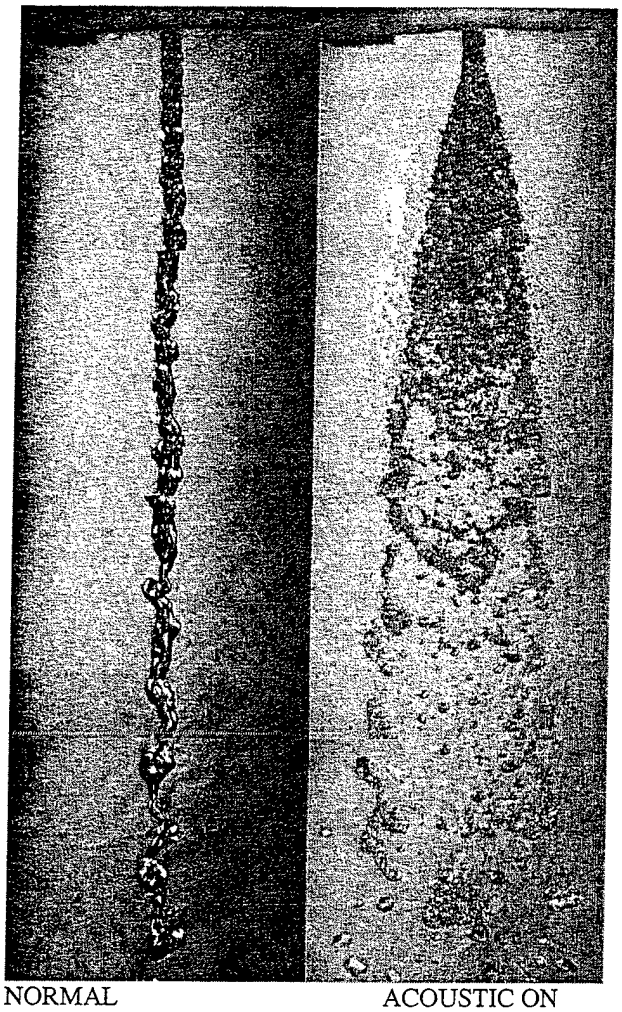

NORMAL ACOUSTIC ON
4800/1.46/150 SIDE

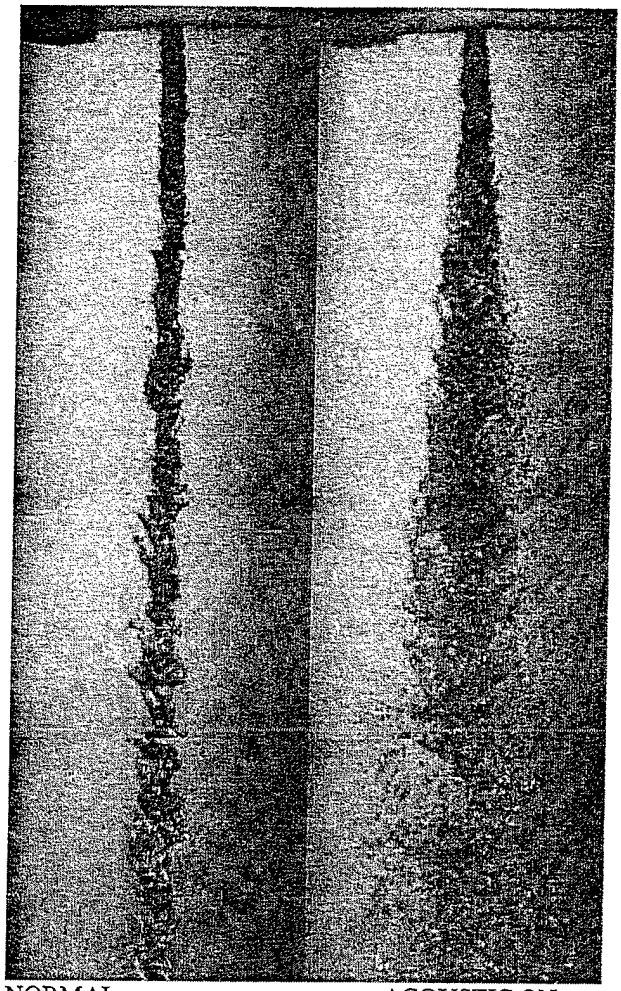

NORMAL ACOUSTIC ON
4800/1.46/500 SIDE

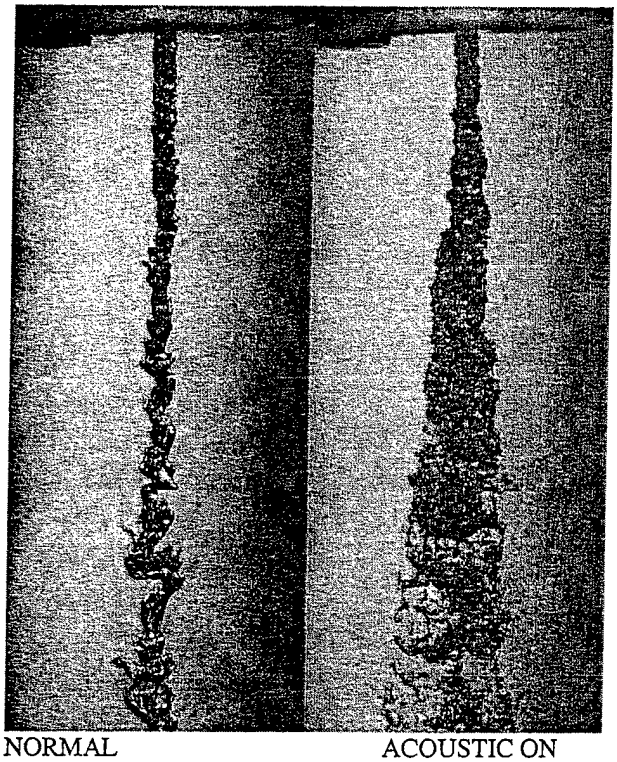

NORMAL ACOUSTIC ON
4800/1.46/300 SIDE

Figure 6. Images of the liquid nitrogen jet injected into the gaseous nitrogen chamber at a subcritical chamber pressure of 1.46 MPa and three different injected flow rates of 150, 300, and 500 mg/s. Acoustic waves are traveling perpendicular and out from the page in these images. The acoustic wave frequency was set at 4800 Hz. Each composite jet image consists of a mosaic of several images taken from the same run but at different times and jet axial locations.

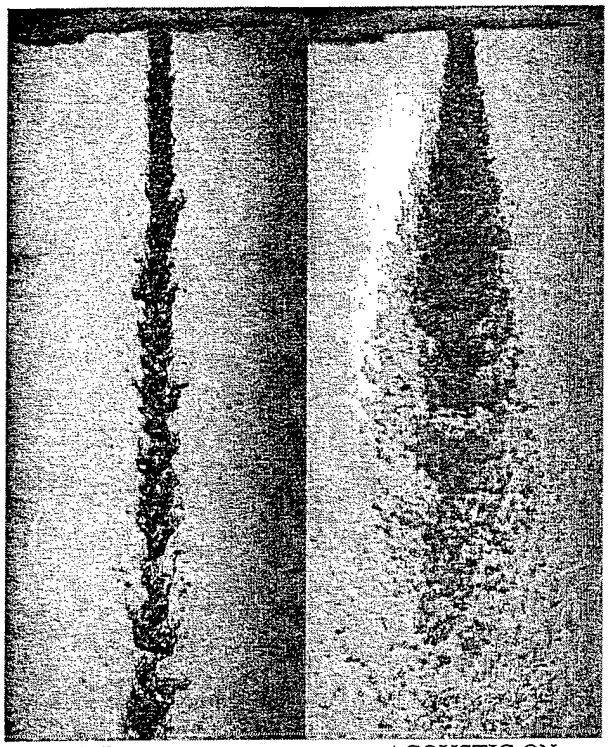

NORMAL ACOUSTIC ON
4800/2.48/150 SIDE

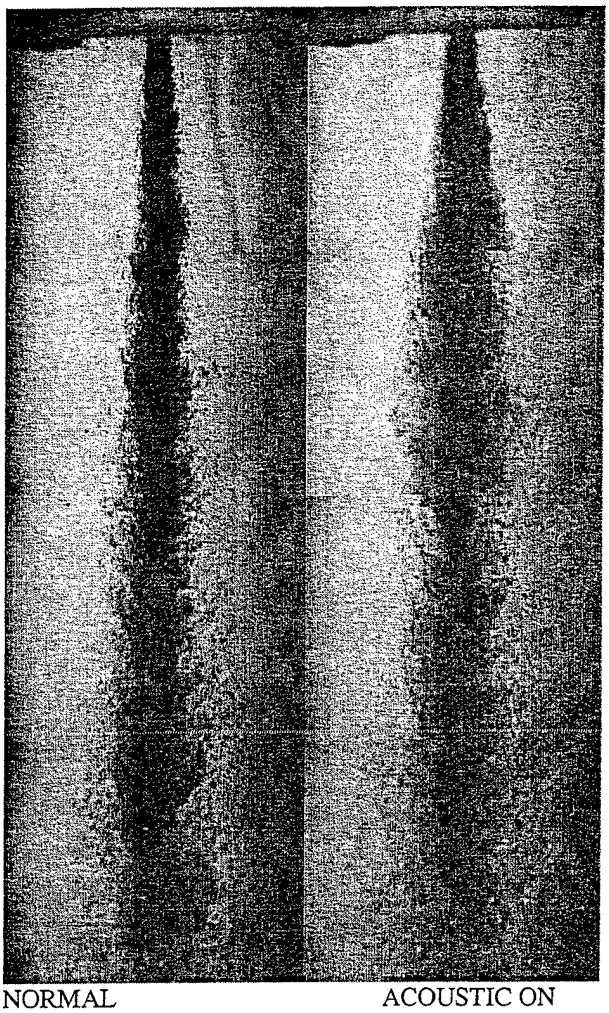

NORMAL ACOUSTIC ON
4800/2.48/500 SIDE

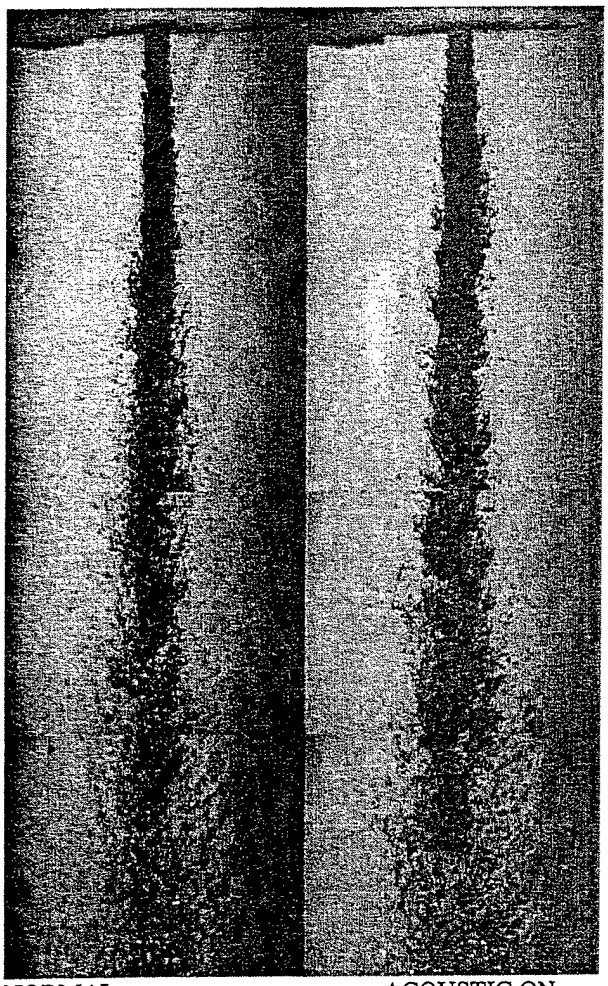

NORMAL ACOUSTIC ON
4800/2.48/300 SIDE

Figure 7. Images of the liquid nitrogen jet injected into the gaseous nitrogen chamber at a near-critical chamber pressure of 2.48 MPa and three different injected flow rates of 150, 300, and 500 mg/s. Acoustic waves are traveling perpendicular and out from the page in these images. The acoustic wave frequency was set at 4800 Hz. Each composite jet image consists of a mosaic of several images taken from the same run but at different times and jet axial locations.

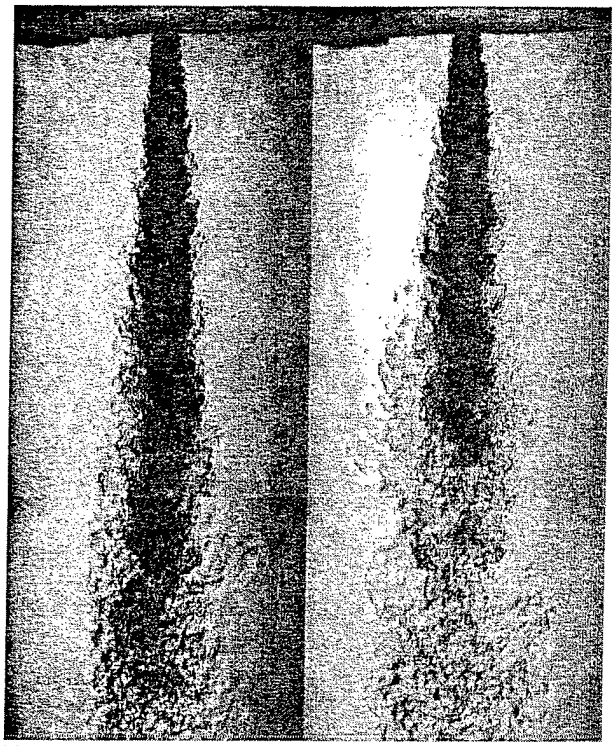

NORMAL ACOUSTIC ON
4800/4.86/150 SEIDE

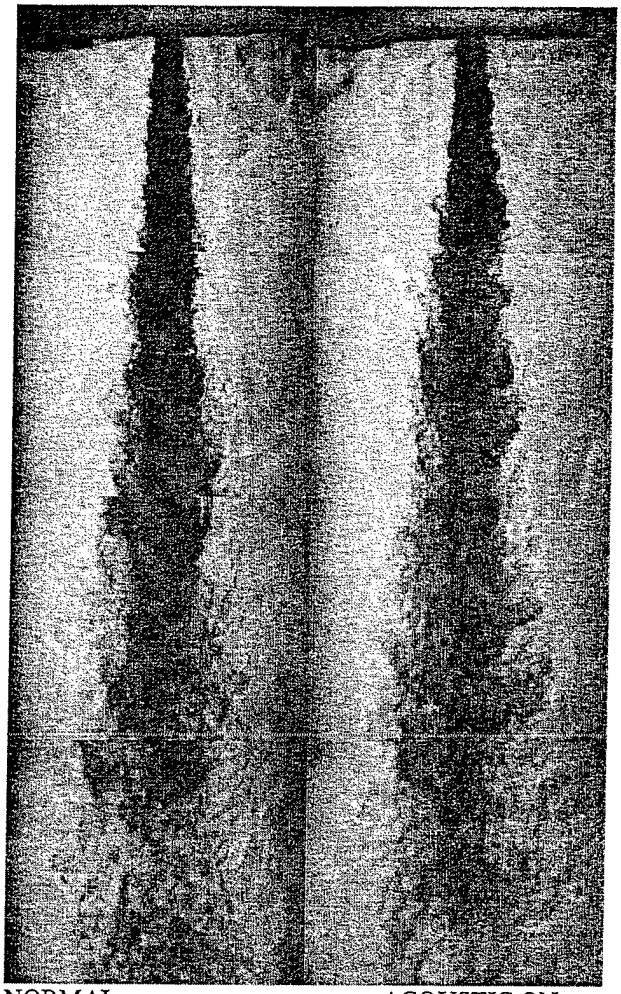

NORMAL ACOUSTIC ON
4800/4.86/500 SEIDE

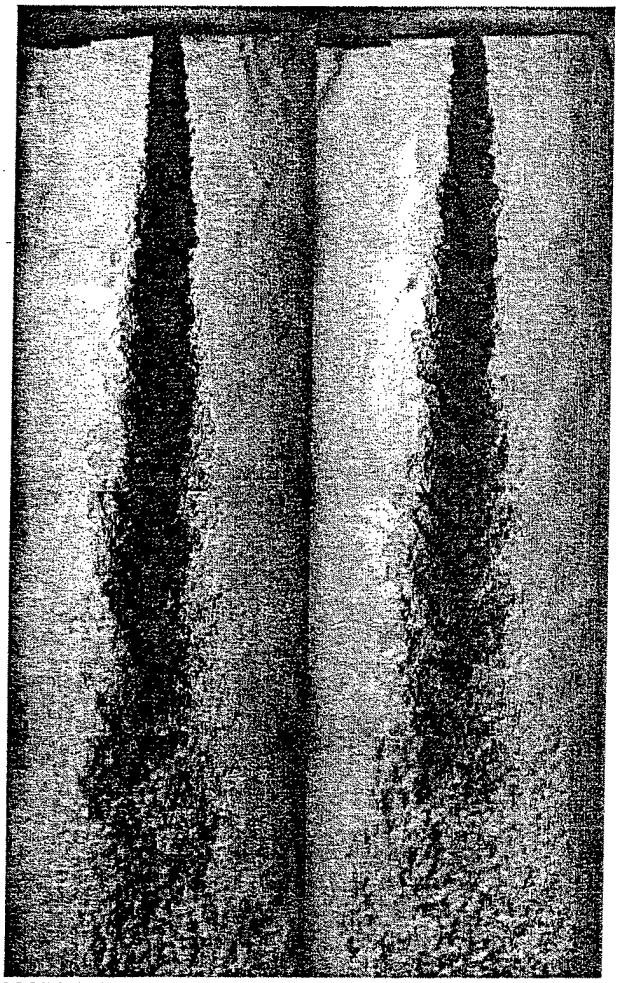

NORMAL ACOUSTIC ON
4800/4.86/300 SEIDE

Figure 8. Images of the liquid nitrogen jet injected into the gaseous nitrogen chamber at a supercritical chamber pressure of 4.86 MPa and three different injected flow rates of 150, 300, and 500 mg/s. Acoustic waves are traveling perpendicular and out from the page in these images. The acoustic wave frequency was set at 4800 Hz. Each composite jet image consists of a mosaic of several images taken from the same run but at different times and jet axial locations.

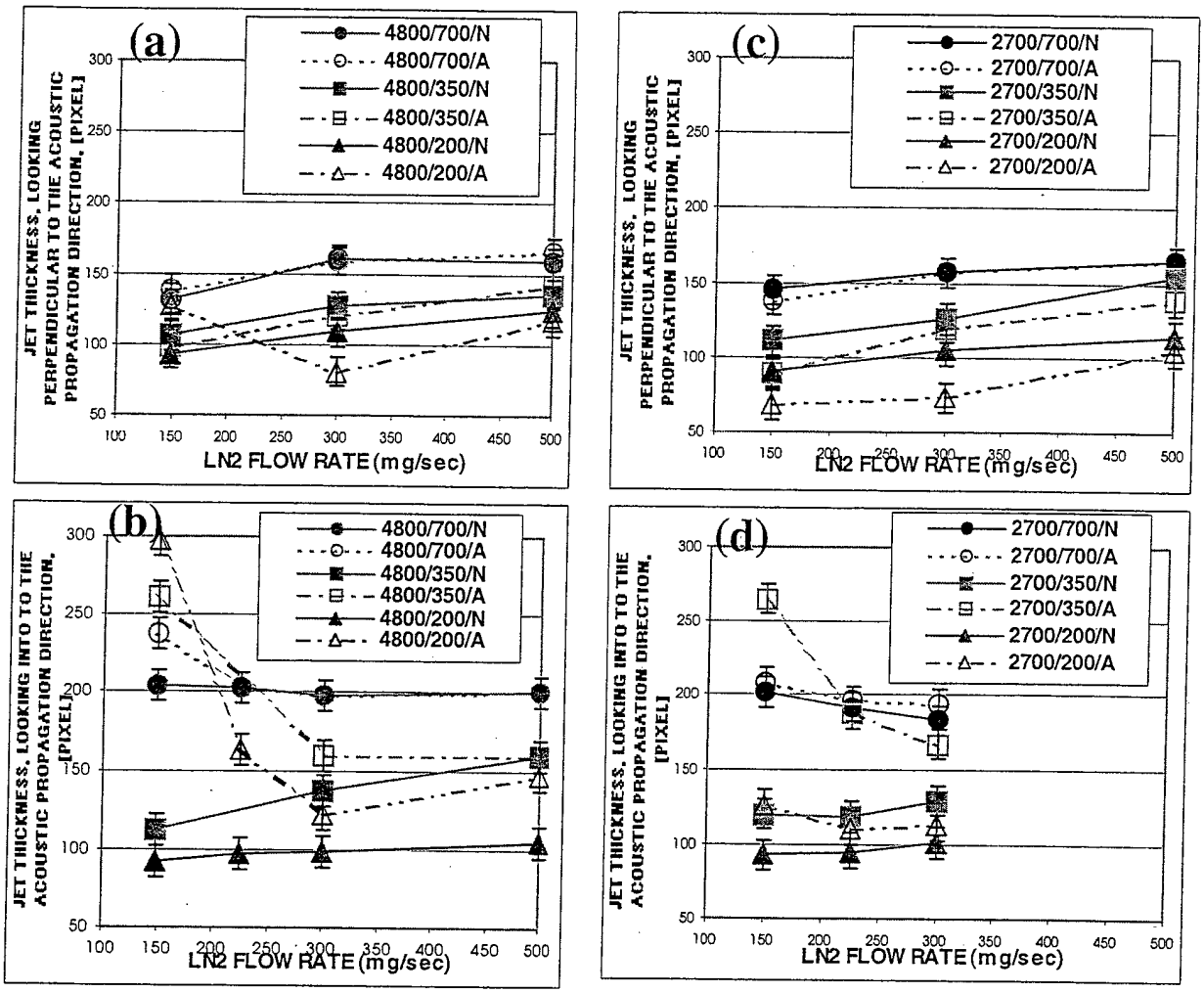

Figure 9. Jet thickness values measured at a distance of 5 injector diameters from the exit and three different flow rates, three chamber pressures, and at two different excitation frequencies of ~2700 and ~4800 Hz. Dashed and solid lines are for with and without presence of acoustic waves respectively. The vertical bar on each symbol indicates the uncertainty of the presented data. The numbers 200, 350, and 700 correspond to chamber pressures of 1.46, 2.48, and 4.86 MPa. The letters N and A refer to the case with and without acoustic waves. LN2 refers to liquid nitrogen. Each image pixel represents approximately 2.82 micron in physical world.

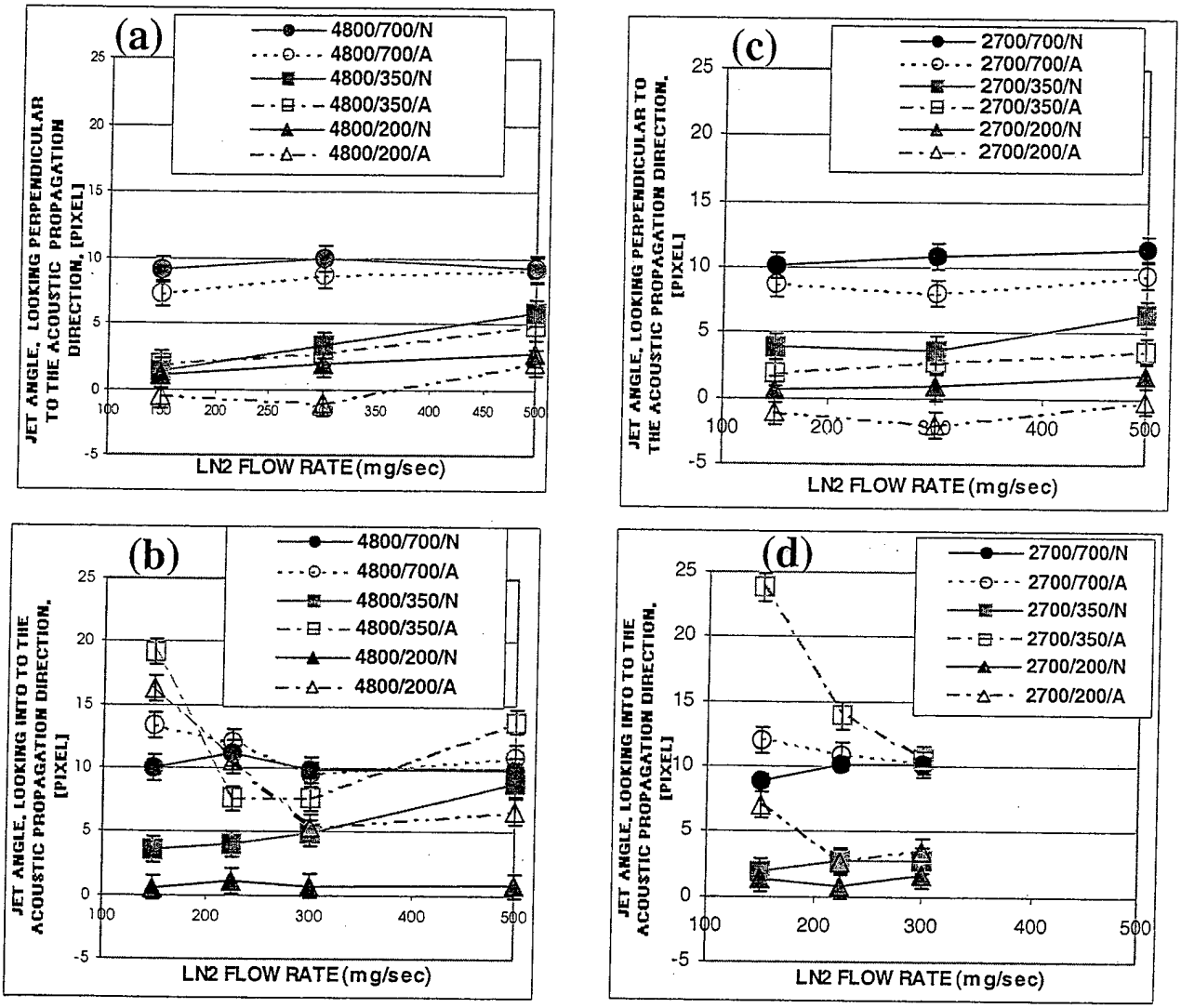

Figure 10. Initial jet angle values measured from information to within about 10 injector diameters from the exit at three different flow rates, three chamber pressures, and at two different excitation frequencies of ~2700 and ~4800 Hz. Dashed and solid lines are for with and without presence of acoustic waves respectively. The vertical bar on each symbol indicates the uncertainty of the presented data. The numbers 200, 350, and 700 psig correspond to chamber pressures of 1.46, 2.48, and 4.86 MPa. The letters N and A refer to the case with and without acoustic waves. LN2 refers to liquid nitrogen. Each image pixel represents approximately 2.82 micron in physical world.